

# Topotecan dynamics, tautomerism and reactivity – $^1\text{H}/^{13}\text{C}$ NMR and ESI MS study

Karolina Hyz,<sup>a</sup> Robert Kawęcki,<sup>a,b</sup> Elżbieta Bednarek,<sup>c</sup> Wojciech Bocian,<sup>a,c</sup> Jerzy Sitkowski<sup>a,c</sup> and Lech Kozerski<sup>a,c\*</sup>



Topotecan (TPT) is in clinical use as an antitumor agent, hycamtin<sup>TM</sup>. Because of this, it requires both biologically and chemically useful information to be available. TPT acts by binding to the covalent complex formed by nicked DNA and topoisomerase I. This has a poisonous effect since inserted into the single-strand nick and TPT inhibits its religation. We used NMR to trace TPT dynamics, tautomerism and solvolysis products in various solvents and conditions. Chemical stability was assessed in methanol and DMSO as compared to water, and the regioselectivity of the *N*- and *O*-methylation was studied using various alkylating agents. The reaction products of quaternization of the nitrogen atom and methylation of the oxygen atom were characterized by means of ESI MS,  $^1\text{H}/^{13}\text{C}$ -HMBC and -HSQCAD NMR. We have focused on the NMR characterization of TPT with an anticipation that its aggregation, tumbling properties and the intramolecular dipolar interactions will be a common feature for other compounds described in this article. These features can also be useful in tracing the interactions of this class of topoisomerase I (TopoI) poisons with DNA. Moreover, the results explained shed light on the recently disclosed problem of lack of stability of TPT in the heart tissue homogenate samples using the analytical assays developed for this class of compounds carried out in the presence of methanol. Copyright © 2010 John Wiley & Sons, Ltd.

Supporting information may be found in the online version of this article.

**Keywords:** NMR; ESI MS; topotecan dynamics; chemical transformations

## Introduction

A continuing interest is observed in the new class of compounds in pursue to find a lead and better formulate an anticancer drug pharmacophore.<sup>[1–5]</sup> Topoisomerases I, II poisons attract much attention in the biomedical research in this direction as they constitute important chemotherapeutic ways in combating cancer.

The cytotoxic plant alkaloid camptothecin (CPT) and the synthetic derivative topotecan (TPT) have emerged as clinically useful anticancer drugs<sup>[6]</sup> and are weakly DNA binding compounds difficult to study by NMR. They are poorly soluble in water at physiological pH, and have strongly pH-dependent  $^1\text{H}$  and  $^{13}\text{C}$  NMR chemical shifts. A lactone-carboxylate equilibrium shown in Scheme 1 is slow on the NMR timescale at room temperature. They act as inhibitors of TopoI<sup>[7–14]</sup> via the formation of stable ternary complexes composed of the drug, DNA and TopoI.<sup>[7,8,15]</sup> The enzyme forms a clamp around a nicked B-form of DNA. The TPT intercalates, stacking with its long axis parallel to the GC(+1).<sup>[16]</sup> An important feature of the binding interaction is the lactone functionality of the TPT, which hydrolyzes to the ring-opened carboxylate form depending on pH (Scheme 1) and is >80% ring-opened at pH 7.4.<sup>[10,11,13]</sup> Despite this, most biological assays indicate that the carboxylate form of TPT is not active as a TopoI inhibitor; on the contrary, the lactone form is stabilized in the presence of DNA.

A thorough understanding of the action mechanism of the drug requires detailed knowledge of its physicochemical properties in the physiological medium. With respect to that, the TPT structure in water at biological pH has not been studied in detail. In addition, with regard to the interaction with DNA, it is important to know

the aggregation state and dynamics of interacting molecules in solution. Our recent studies<sup>[17,18]</sup> and the present results indicate clearly that TPT is in a form of aggregates in a buffered water solution and tumbles slowly. All protons are shifted to lower frequencies in the self-association state, consistent with the expected stacked structure. The intermolecular NOEs, observed for the distant protons (see Table 2, for example from 23-CH<sub>2</sub> to 19-CH<sub>3</sub>, etc.) suggest head-to-tail stacking of the TPT molecules in aggregates.

The self-association binding constant of the TPT, calculated from the present DNMR results, *ca*  $3.3 \pm 1 \text{ mM}^{-1}$  (see Supporting Information) is consistent with our earlier results obtained from dilution studies and earlier published UV experiments.<sup>[19]</sup> We have also found that the carboxylate form binds *ca* 40 times weaker than the lactone form to the nicked DNA decamer, in agreement with the biological assays.<sup>[18]</sup>

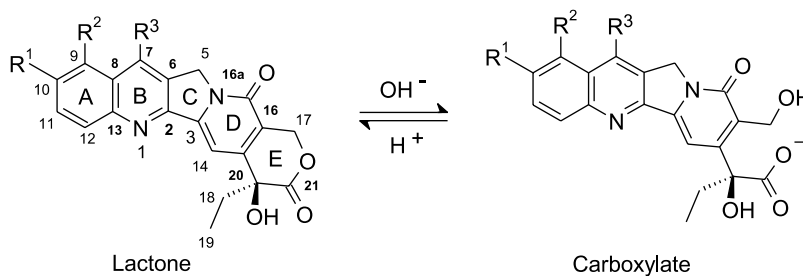
In Scheme 1, the two most important constituents of the equilibrium are shown, which are observed in the NMR spectrum in buffered water solutions at a wide pH range of 5–8. We characterized these two forms of TPT in solution and have

\* Correspondence to: Lech Kozerski, Institute of Organic Chemistry, Polish Academy of Sciences, 01-224 Warsaw, Kasprzaka 44, Poland.  
E-mail: lkoz@icho.edu.pl

a Institute of Organic Chemistry, Polish Academy of Sciences, 01-224 Warszawa, Kasprzaka 44, Poland

b Institute of Chemistry, University of Podlasie, ul. 3 Maja 54, 08-110 Siedlce, Poland

c National Medicines Institute, 00-725 Warszawa, Chełmska 30/34, Poland



**Scheme 1.**  $R^1 = H, R^2 = H, R^3 = H$  [camptothecin];  $R^1 = OH, R^2 = {}^{23}\text{CH}_2\text{N}({}^{22}\text{CH}_3)_2, R^3 = H$  [topotecan];  $R^1 = 1\text{-}[4'\text{-pipridynyl-piperidine}] \text{ carboxy}, R^2 = H, R^3 = \text{C}^2\text{H}^5$  [irinotecan].

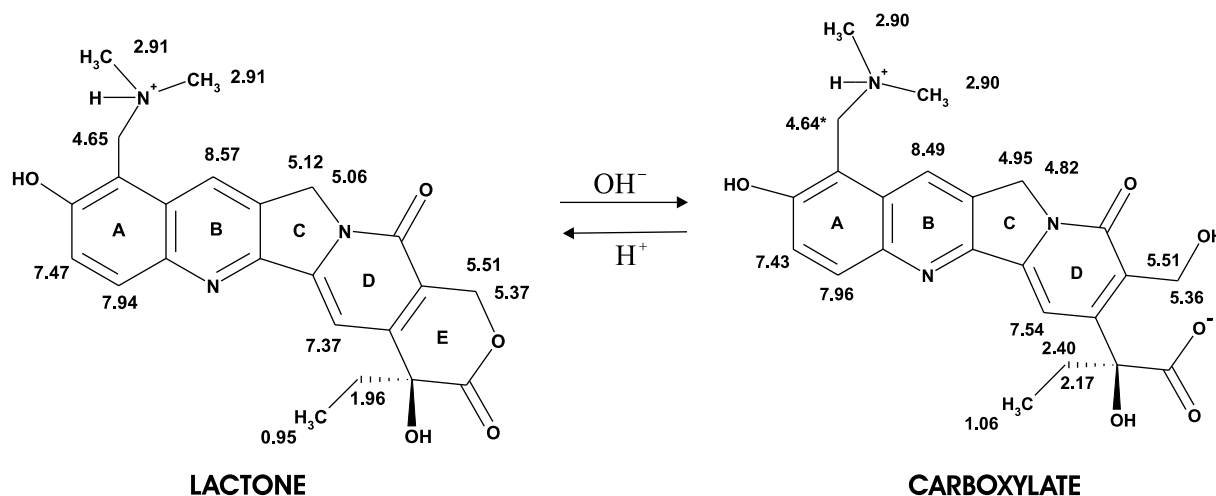
presented their dynamics in water, in conditions close to physiological. In addition, we gave an evidence for a tautomer, an enol form shown in Scheme 3, which, in contrast to the lactone and carboxylate forms, is observed in water and methanol solutions as intermediate species. We also determined the molecular tumbling parameters of a lead compound in this class of the Topol inhibitors, TPT in water. Moreover, the intramolecular NOEs were established as a reference data set useful in tracing the intermolecular contacts with DNA as targets. We focused on the TPT with an anticipation that its tumbling properties and the intramolecular dipolar interactions will be a common feature for the other compounds described in this article. The alkylation products of the nitrogen or oxygen sites, formed under various conditions, were characterized by ESI MS,  ${}^1\text{H}/{}^{13}\text{C}$ -HMBC and -HSQCAD NMR.

These results shed light on the recently disclosed problem of lack of the TPT stability in the heart tissue homogenate samples<sup>[20,21]</sup> using methanol in the analytical assays developed for this class of compounds.

## Results and Discussion

### Structure of TPT $\times$ HCl in water

The structure in water, as being close to physiological medium, is of primary importance. At pH 4.5, after dissolving, TPT  $\times$  HCl is *ca* 95% in the lactone form [see Scheme 2), chemical shifts are pH-sensitive (compare data in Table 3 at pH 6.0)]. We studied  ${}^1\text{H}$ - $T_1$  relaxation times and NOE to address the aggregation state and the molecular tumbling in this medium.



**Scheme 2.**  ${}^1\text{H}$ -chemical shifts of TPT  $\times$  HCl in  $\text{D}_2\text{O}$ , pH 4.5.

### ${}^1\text{H}$ - $T_1$ relaxation times and NOE enhancements

In order to evaluate the correlation time for the TPT and intramolecular NOEs in buffered water solution at pH 5,  $T_1$  and NOE measurements were performed at room temperature and at 13 and 3 °C. As a reference, a TPT solution in  $\text{DMSO-}d_6/\text{CDCl}_3$  (2 : 4, v/v ratio) was also studied (Table S2, Supporting Information).

The change of  $T_1$  values with the temperature variation is a sensitive gauge of the molecular tumbling and, indirectly, of the state of aggregation. We do not intend to quantitatively discuss the absolute  $T_1$  values of aromatic *versus* aliphatic protons. This is because different relaxation mechanisms can dominate in both, i.e. chemical shift anisotropy for the protons attached to the extended aromatic plane and spin rotation for the side methyl groups. The data cited in Table 1 clearly show the characteristic tendencies for large molecules outside the extreme narrowing regime. With decreasing temperature, the  $T_1$  of the ring protons 7-H, 12-H, 11-H and 18- $\text{CH}_2$  increases whereas for the 19- $\text{CH}_3$  protons, it is essentially constant and shows the opposite trend for the dimethylamino group. These results indicate that the main skeleton protons are characterized by the  $\omega\tau_c \gg 1$ , i.e. fall into regime of large molecules which exhibit the negative NOEs. The side group has apparently a much shorter correlation time and its rotational correlation time is characterized by the condition  $\omega\tau_c \ll 1$ , observed in the region of extreme narrowing and positive NOEs. Lowering the temperature is accompanied by the increase in the solvent viscosity. This effect should result in shortening of all relaxation times, likewise the aggregation, whereas opposite trends are still clearly visible. Therefore, the

**Table 1.** Comparison of the  $T_1$  relaxation times in TPT at different temperatures in buffered  $D_2O$  solution<sup>a</sup>

Proton/ Temperature	$T_1$ (s)		
	30 °C	13 °C	3 °C
7-H	0.72 ± 0.10	0.89 ± 0.03	0.97 ± 0.03
12-H	1.93, 2.01 ± 0.54	2.40, 2.45 ± 0.11	2.37, 2.34 ± 0.09
11-H	1.76, 1.89 ± 0.44	2.34, 2.41 ± 0.11	2.37, 2.47 ± 0.11
14-H	2.91 ± 0.65	3.08 ± 0.13	2.70 ± 0.11
Nme <sub>2</sub>	0.51, 0.52 ± 0.01	0.44, 0.44 ± 0.01	0.41, 0.41 ± 0.01
18-CH <sub>2</sub>	0.34, 0.35 ± 0.03	0.43, 0.43 ± 0.01	0.49, 0.50 ± 0.01
19-CH <sub>3</sub>	0.72 ± 0.10	0.89 ± 0.03	0.97 ± 0.03

<sup>a</sup> The solution of 0.3 mg of TPT in 600  $\mu$ l  $D_2O$  buffer; 50 mM in NaCl, 50 mM in  $K_3PO_4$ , pH 5. Signals close to water; 5, 23, 17-CH<sub>2</sub> are not cited. The  $T_1$  relaxation times are cited for each component of multiplet.

observed effects cannot be attributed solely to the increase of solvent viscosity and/or aggregation but also, as expected, to different correlation times of the skeleton and side groups in the molecule. This is evident from comparison of the  $T_1$  values at 30 and 13 °C whereas the comparison of the values at 13 and 3 °C suggests that both contributions compete effectively. While we do not attempt to quantify individual shares of each effect, we only state qualitatively that these experiments suggest that at ambient temperatures, and in a buffered water solution, the TPT molecules form molecular clusters. These clusters tumble slowly in solution which should give rise to nulled NOEs.

In Table 2, the steady state NOEs for  $D_2O$  solution of TPT at 30, 13 and 3 °C are listed. DPGFSE NOE<sup>[22]</sup> and ROE data are cited at 30 °C for comparison. As expected, Table 2 shows that in  $D_2O$  solution at 30 °C, the intramolecular effects are nearly nulled and at the same time intermolecular NOEs appear for all parts of the TPT molecule. The selective DPGFSE ROE in a few cases show larger positive intramolecular effects, in contrast to DPGFSE NOE performed with the same timing. With decreasing temperature, both intramolecular (11-H vs 12-H) and intermolecular effects tend to be larger and negative. This is a clear evidence that self-association of TPT in buffered  $D_2O$  solution occurs even at very low concentrations. The change of NOE from a small positive value at 30 °C to a negative one at 13 °C evidences that the molecular tumbling of TPT cluster approaches the correlation time characteristic for biomolecules. This also confirms that these molecular clusters have the rotational correlation time, at ambient temperatures and at 500 MHz, fulfilling the condition  $\omega_0\tau_c \approx 1.12$  giving the correlation time,  $\tau_c$ , of the order of  $3.55 \times 10^{-10}$  s.

The reference sample in  $CDCl_3/DMSO-d_6$ , 4:2 v/v shows no steady state NOE effects at room temperature whereas DPGFSE ROE (Table S2) shows expected intramolecular effects but no intermolecular effects. Theoretical intramolecular NOEs are given for comparison. They were calculated using the geometry and interproton distances as obtained using protocol described previously.<sup>[23,24]</sup> Table S3 shows the comparison of the spectral parameters obtained after the experiments were carried out in water and  $DMSO-d_6/CDCl_3$  solutions of TPT. There are negligible differences in chemical shifts despite the difference of dielectric constants of both solvents. Although it is unexpected, the TPT chemical shifts are insensitive to the solvent and concentration changes.

The above experiments suggest the aggregation of TPT in buffered water solution at ambient temperatures. The slow molecular tumbling of highly solvated monomeric molecule, although possible theoretically, is less probable in the case of low molecular weight structure (MW = 421). The observed long-range effects, for example, from 11-H to 18-CH<sub>2</sub>, (Table 2) interpreted here as intermolecular effects, can, in principle, be seen as spin diffusion artefacts. Again, this is highly unlikely due to the fact that both groups are very distant in a molecule and there is no intervening proton between them which might ease the spin diffusion.

With regard to the problem of aggregation, an earlier paper cites the self-association binding constant for irinotecan  $2.41 \times 10^4$  [ $M^{-1}$ ], forming dimers at the level of 2 mM in water, as obtained from UV spectra.<sup>[25]</sup> In a recent paper, we have established that the self-association constant  $K_a^{TPT} = 3.4 \times 10^3$  [ $M^{-1}$ ] from the concentration dependence of TPT chemical shifts.<sup>[17]</sup> In the Supporting Information, the temperature dependence of TPT chemical shifts is given, which were obtained from the DNMR experiment performed in this work and yield the self-aggregation constant of  $ca K_a^{TPT} = 3.0 \times 10^3$  [ $M^{-1}$ ]. The intermolecular NOEs seen in Table 2 suggest head-to-tail orientation of TPT molecules in aggregate. A more detailed analysis of the aggregate geometry was not attempted because the observed NOEs are very small and, in addition, they are derived from conformational ensemble in fast exchange.

We present this information which can have application in biological studies, DNA binding experiments and pharmaceutical tests for medicine bioavailability.

### TPT structure in $CD_3OD$ solution

The information on the medicinal behavior in different solvents is important for biological assays and pharmaceutical formulations. Methanol is used in the analytical assays for the heart tissue homogenate samples developed for this class of compounds. For this reason, we present the TPT reactivity in this solvent in the following.

Two chemical processes are disclosed in  $CD_3OD$  solution of TPT  $\times$  HCl which have very different time dependencies, i.e. substitution of the  $-NHMe_2^+ Cl^-$  group yielding 23-CH<sub>2</sub>-OCD<sub>3</sub>, Fig. 1, and deuteration of 5-CH<sub>2</sub> group which undergoes through intermediate enol species formation as shown in Scheme 3 and Fig. 2. Figures 1 and 2 show that the  $NHMe_2^+ Cl^-$  group substitution is completed within 10 days and is displayed by the spectral process evidence presented in Fig. 1. The most diagnostic feature of the process is the disappearance of the signal at  $\delta = 4.78$  ppm (23-CH<sub>2</sub>-N) and the rise of the signal at  $\delta = 5.01$  ppm (23-CH<sub>2</sub>-O). Another clue is the disappearance of the signal due to  $Me_2ND^+ Cl^-$  group and the rise of the signal at 2.72 ppm, due to  $Me_2ND_2^+ Cl^-$  group. This process is also readily confirmed by high-frequency shift of both nuclei in the 23-<sup>13</sup>C<sup>1</sup>H<sub>2</sub> group with respect to their positions in parent TPT  $\times$  HCl (Table 3). It can also be deduced from the data (Table 3) that the ether is in the lactone form. This is done by comparing its 21-<sup>13</sup>C = O chemical shift and the lack of proton non-equivalence in 18-CH<sub>2</sub> group which is characteristic for carboxylate but not for the lactone form in all solvents used.

Sanna *et al.*<sup>[26,27]</sup> have postulated the amide–enaminoenol tautomerism on rings C/D junction at pH < 4 on the basis of theoretical calculations, but it was not documented experimentally. We have observed that after prolonged standing of TPT  $\times$  HCl

**Table 2.** Comparison of the NOE enhancements in TPT in buffered water solution at different temperatures<sup>a</sup>

Proton irradi.	Proton observed NOE (%)						
	7-H	12-H	11-H	14-H	23-CH <sub>2</sub>	18-CH <sub>2</sub>	19-CH <sub>3</sub>
7-H	7-H	-1.0	-0.9	-1.5	(0; 16.9)	-	-
	*	-	-1.3	-1.0	-	-0.6	-1.0
12-H		-1.6	-2.5	0.7	-19.6	-	-0.8
	-0.6		-1.1(-1.0; 10.8)	-3.2		-2.4	-1.5
	-1.2	*	-18.4	-3.2		-3.7	-2.9
11-H	-3.2		-33.7	-4.5	-8.2	-3.1	-2.0
	2.9	1.2(0.8; 7.0)		-4.9		4.1	3.2
	-0.5		*	-4.0		-	0.5
14-H	-0.7	-29.3		-5.6		2.0	-1.1
	2.9	1.4	-			2.8	2.7
	2.1	0.4	-0.8	*			0.6
23-CH <sub>2</sub> <sup>b</sup>		-1.4	-5.9		-5.9	0.4	0.9
	-	-	-	-	*	-	-
	-54.9	-7.3	-8.9	-3.2		-3.0	-2.4
18-CH <sub>2</sub>	0.5	0.2	0.9	3.5			5.7(3.8; 7.0)
		-1.6		-2.3		*	0.4
	-1.4	-2.1	-6.7	-6.7			-4.9
19-CH <sub>3</sub>	1.2	1.1	1.1	3.9		4.0(2.3; 3.5)	
	-2.7	-3.3	-1.9	-3.1		-1.8	*
		-	-3.4	-6.8		-2.1	

<sup>a</sup> The DPGSE NOE and ROE are cited at 30 °C for comparison (round brackets). The solution of 0.3 mg TPT in 600 μl D<sub>2</sub>O buffer; 50 mM in NaCl, 50 mM in K<sub>3</sub>PO<sub>4</sub>, pH 5. The values are cited from the top to the bottom at 30, 13 and 3 °C, respectively. Positions not cited have less than 0.4 absolute value effect. 23-CH<sub>2</sub> resonance was not irradiated at 30 and 13 °C due to the overlap with residual HOD signal. Although the precision of the NOE enhancements is less than a tenth, we present them here in this precision in order to have better comparison of temperature effect on NOEs. The data are not used for structural assessments.

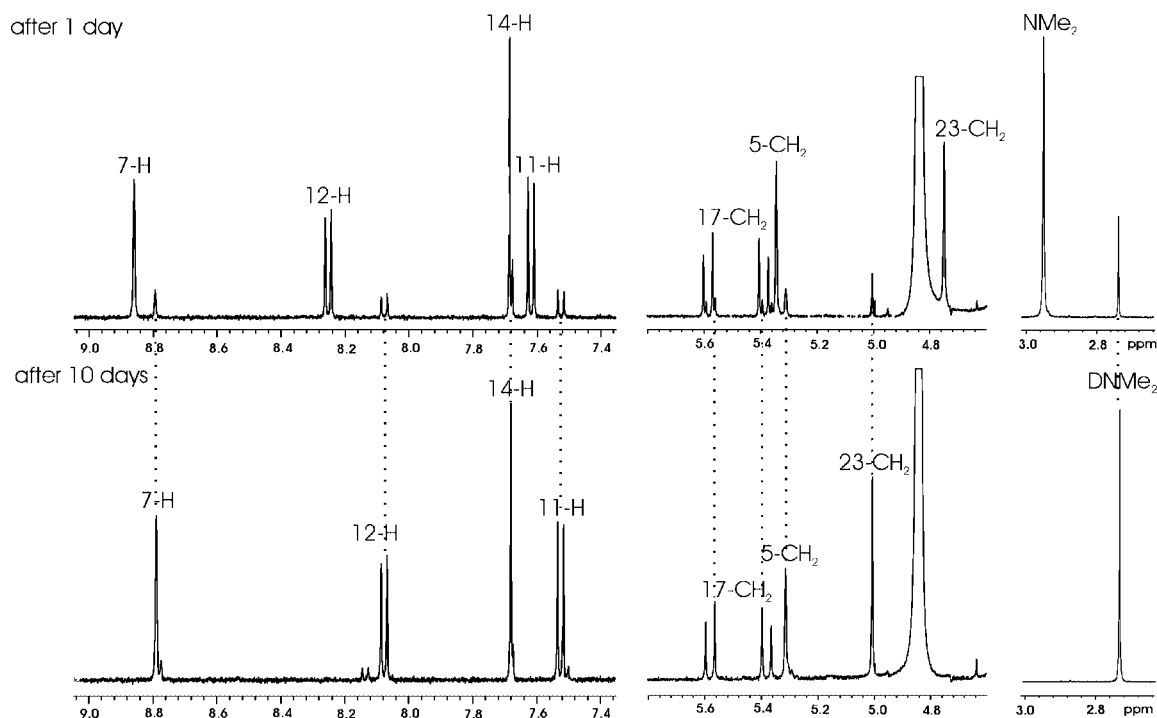
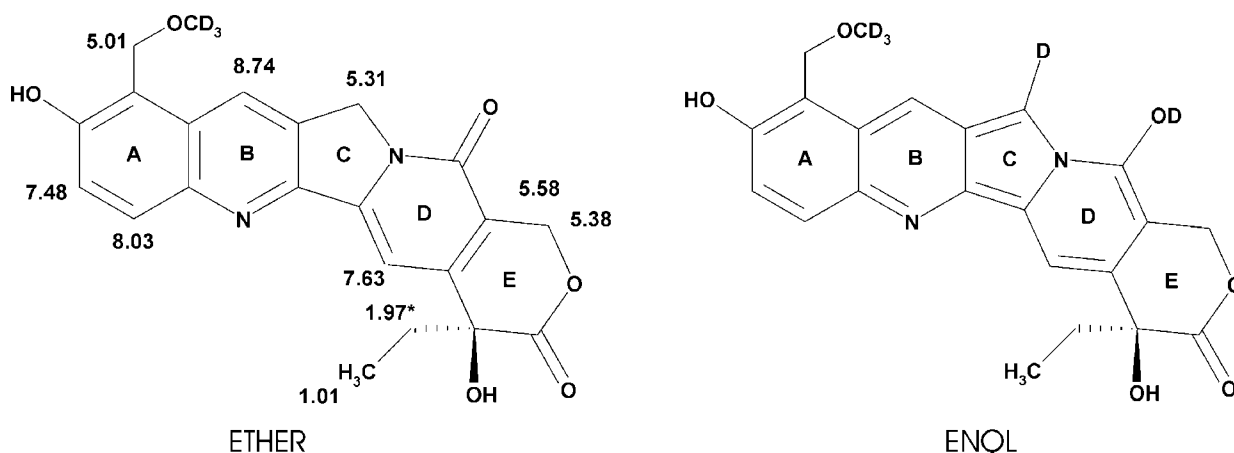


**Figure 1.** Time dependence of the  $\text{-NDMe}_2^+ \text{Cl}^-$  substitution in TPT  $\times$  HCl in CD<sub>3</sub>OD. The presence of the OCD<sub>3</sub> group is evidenced in the HMBC spectrum.



**Scheme 3.** ETHER form as a product of deuteration in methanol- $d_4$  and an ENOL form as intermediate species in deuteration of TPT  $\times$  HCl.

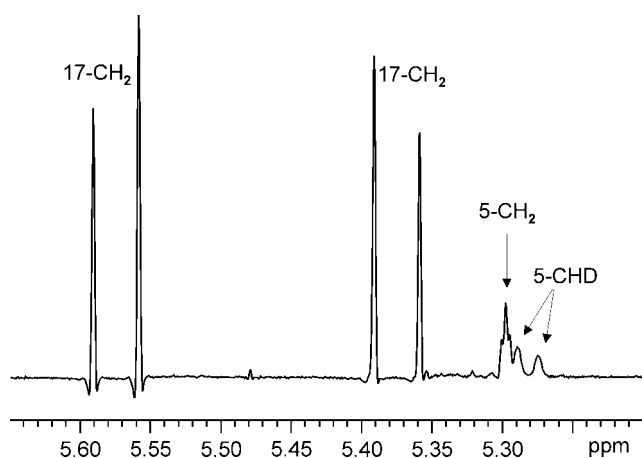


**Figure 2.** The 5 ppm region of the  $^1\text{H}$  NMR of spectrum of TPT  $\times$  HCl in  $\text{CD}_3\text{OD}$  after a few weeks.

in methanol- $d_4$  solution, the 5- $\text{CH}_2$  signal disappears gradually and after few months, the process of deuteration is nearly complete (Fig. 2).

This can be interpreted as a result of the presence of the enol-type tautomer shown in Scheme 3. This tautomer is present only as an intermediate species, most probably due to its higher energy than that of the parent amide. The dynamics of this process is very slow. This confirms the theoretical calculations according to which there is an energy difference of 100 kJ/mol in favor of the keto form.<sup>[27]</sup>

Interestingly, both processes are not observed instantaneously in  $\text{D}_2\text{O}$  solution at pH  $\sim$ 6.

The bottom spectrum in Fig. 1 shows also the second set of signals which is tentatively assigned to the carboxylate form which cannot be characterized due to its very small population.

Figure 2 shows the spectral result of the second process, i.e. 5- $\text{CH}_2$  deuteration proceeding via intermediate enol (Scheme 3). The triplet at  $\delta = 5.3$  ppm is a residual di-hydrogenated 5- $\text{CH}_2$  group characterized by  $^2J_{\text{gem}} = -19$  Hz,  $\Delta\nu_{\text{gem}} = 8$  Hz, and long-range couplings to H-7, 0.9 Hz. The two broad, low-frequency signals are due to stereoselectively monodeuterated 5-CHD groups; each signal is characterized by reduced  $^2J_{\text{gem}}/6.52$  Hz geminal coupling, spin coupling to deuterium and long-range coupling to 7-H proton. The simulation of the full spin system

comprising 5- $\text{CH}_2$ , 7-H, 11-H and 12-H protons is shown in Figure S1.

#### Reaction of TPT on silica in ethyl acetate/methanol

TPT  $\times$  HCl cannot be purified using silica gel. The reaction described above in methanol- $d_4$  proceeds instantaneously on developing the silica plates with ethyl acetate/methanol (4:1, vol%). Silica catalyzes the elimination reaction which results in TPT derivatization yielding an ether 23- $\text{CH}_2\text{OCH}_3$ . The compounds are characterized in Table 3 by  $^1\text{H}$  and  $^{13}\text{C}$  NMR; Table 3 comprises the data for the various TPT forms in the studied media.

#### Quaternization reactions of TPT by various alkylating agents

Following the clinical application of the Hycamtin<sup>®</sup> and Camptosar<sup>®</sup> (TPT and irinotecan, respectively, Scheme 1) several groups became interested in structural modifications of CPT<sup>[3,28,29]</sup> with the goal to improve its water solubility and cytotoxicity *versus* tumor cells. We have attempted to synthesize the quaternary trimethylammonium salt using  $\text{CH}_3\text{SO}_2\text{OCH}_3$  and  $\text{CF}_3\text{SO}_2\text{OCH}_3$  as alkylating agents. It turned out that, in case of these reagents, the reaction was completed, yielding *ca* 10–50% of trimethylammonium salts. In addition, the reaction yielded at least two other types of TPT derivatives, i.e. expected *N*-methylation and double methylation, 23-*N* and 10-*O*, or 20-*O* doubly methylated products (*m/z* 450). More importantly, *N*-methylated product, characterized after workup of reaction mixture by MS (*m/z* 436.1) and  $^1\text{H}/^{13}\text{C}$ -HSQCAD, -HMBC NMR, turned out to be unstable. For this reason, we did not attempt to separate the individual compounds but assigned their structures using ESI MS,  $^1\text{H}$  NMR, and HSQCAD and  $^1\text{H}/^{13}\text{C}$ -GHMBC NMR in  $\text{DMSO}-d_6$  solution. Figure 3 and Scheme 4 show the  $^1\text{H}$  NMR spectra which were used in spectral assignment and the structures with assigned proton/carbon resonances, respectively. We have labeled compounds in the reaction mixture according to product structure.

Each structure in Scheme 4 is confirmed by a few cross-peaks which characterize the polarization transfer in HMBC spectrum used to connect given 23- $\text{CH}_2$  group to the carbon atom in ring A, 10-C. The assignment of the structures is accomplished with the aid of a spectrum of TPT  $\times$  HCl in  $\text{DMSO}-d_6$  which shows the alcohol after standing several months. The other parts of the spectra are shown in Fig. S1 (3.5–5.5 ppm region)

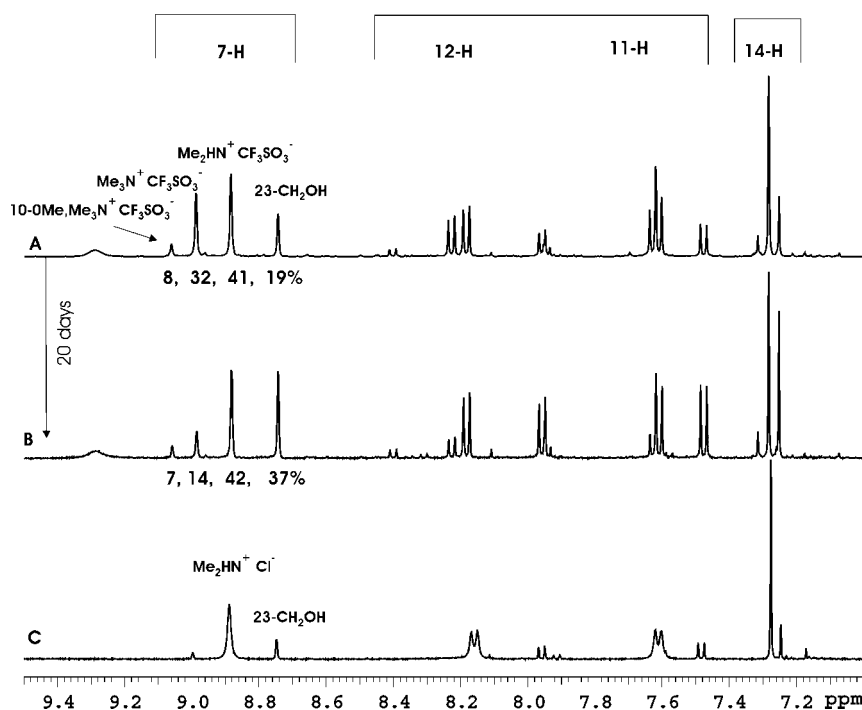


**Figure 3.** The aromatic part of the  $^1\text{H}$  NMR spectrum of the product mixture (DMSO- $d_6$  solution) in the quaternization reaction of neutral TPT with  $\text{CF}_3\text{SO}_2\text{OCH}_3$ , spectrum A. The product composition after 1 month reaction, spectrum B. The TPT  $\times$  HCl spectrum in DMSO- $d_6$ , a month after dissolving, is shown for comparison, spectrum C. The signals are labeled with the acronyms characterizing the type of changes in ring A.

and Fig. S2 (0.3–3.3 ppm region). The structural evidence of the  $[\text{Me}_3\text{N}^+ \text{CF}_3\text{SO}_3^-]$  salt and  $[\text{10-O-Me, Me}_3\text{N}^+ \text{CF}_3\text{SO}_3^-]$  salt is backed by the presence of signal at 3.12 ppm belonging to  $\text{Me}_3\text{N}^+$  group (Fig. S2), and  $^1\text{H}$  and  $^{13}\text{C}$  NMR chemical shifts (Scheme 4). The chemical process which is evidenced in Fig. 1 is the substitution in the  $[\text{Me}_3\text{N}^+ \text{CF}_3\text{SO}_3^-]$  salt at 23-C position, yielding the alcohol 23- $\text{CH}_2\text{OH}$  and the  $[\text{Me}_3\text{HN}^+ \text{CF}_3\text{SO}_3^-]$  salt (Fig. S2, doublet at 2.73 ppm). Interestingly, in the  $[\text{Me}_2\text{HN}^+ \text{CF}_3\text{SO}_3^-]$  salt, this substitution in the  $[\text{Me}_2\text{HN}^+ \text{CF}_3\text{SO}_3^-]$  group does not proceed so easily, as confirmed by the presence of negligible amount of alcohol in spectrum C representing the process of  $[\text{Me}_2\text{HN}^+ \text{Cl}^-]$  salt incubation in DMSO- $d_6$  for few months.

In Fig. 4, the  $^1\text{H}/^{13}\text{C}$ -HMBC evidence for the structure of the  $[\text{Me}_3\text{HN}^+ \text{CF}_3\text{SO}_3^-]$  salt of TPT in solution is presented. The  $^1\text{H}/^{13}\text{C}$ -HMBC evidence for the structure of the  $[\text{Me}_3\text{N}^+ \text{CH}_3\text{SO}_3^-]$  salt of TPT in solution is presented in Fig. 5.

Figure 5 shows the long-range correlation from methyl groups in  $(^{13}\text{CH}_3)_3\text{N}^+ \text{CH}_3\text{SO}_3^-$  ion pair ( $\delta = 3.11/\delta = 53.1$  ppm and  $\delta = 3.05/\delta = 45.5$  ppm for cation and anion, respectively) to 23- $\text{C}^1\text{H}_2$  methylene group ( $\delta = 53.9$  ppm) identified in the  $^1\text{H}$  trace at  $\delta = 4.93$  ppm. In addition to that, the methyl group,  $(\text{C}^1\text{H}_3)_3^{14}\text{N}^+$ , in trimethylammonium salt, at  $\delta 3.11$  ppm, is easily identified by small coupling,  $^3J(^1\text{H}, ^{14}\text{N})$  ca 2 Hz to  $^{14}\text{N}$  nucleus, often observed in nitrogen quaternary salts due to symmetric environment of nitrogen atom.

With respect to the above evidence of structure, we were not able to reconcile it with the result which cites the chemical shift of  $(\text{CH}_3)_3\text{N}^+$ -group at  $\delta = 2.94$  ppm and  $\text{CH}_3\text{SO}_3^-$  at  $\delta = 2.78$  ppm for the same compound but in methanol/ $\text{CDCl}_3$  solution (vol. ratio not given) with no information on  $^{13}\text{C}$ .<sup>[30]</sup> Our experience is that in methanol solution the quaternary salt is not stable.

## Conclusion

The tautomeric structure and stability in solution, in different media  $\text{CH}_3\text{OH}$ , DMSO and water, has been established for the Topol inhibitor in clinical use, hycamtin<sup>®</sup>. We have shown in the present work that TPT tumbles in water solution as aggregate with the correlation time characteristic for large molecules at decreased temperature, ca 5 °C, but gives nulled NOEs, both in water or DMSO- $d_6$ / $\text{CDCl}_3$  solutions at room temperature. The TPT  $\times$  HCl is unstable in  $\text{CH}_3\text{OH}$  solution and two processes were disclosed, i.e. substitution of the  $(\text{CH}_3)_2\text{HN}^+$ -group yielding the ether 23- $\text{CH}_2\text{-OCH}_3$  and the presence of enamine-enol form (Scheme 2) at ring C/D junction. This was evidenced by the deuteration of the 5- $\text{CH}_2$  group. This is the first experimental evidence of the existence of this type of tautomer, which was earlier predicted theoretically.<sup>[25]</sup> The alkylation of neutral TPT using  $\text{CF}_3\text{-SO}_2\text{-OCH}_3$  yields 10-*O*-, 20-*O*- and 22-*N*-alkylated products, and *N,O*-doubly methylated products with the predominance of the latter, i.e. 22-*N*-alkylated product. The simultaneous presence of both *N*-dimethylammonium- and *N*-trimethylammonium-triflates in DMSO- $d_6$  solution allows the observation that the latter is much more susceptible to substitution. Present results on the TPT instability in methanol give an explanation for the observed degradation of TPT in the heart tissue homogenates on storage at room temperature in methanol for an extended period of time.<sup>[21]</sup> Further studies on the chemistry of derivatives of the CPT family are in progress.

## Experimental

TPT hydrochloride was purchased from Alexis Biochemicals and was used directly without applying any additional purification steps. To obtain free base TPT, TPT hydrochloride (2 mg,

**Table 3.**  $^1\text{H}$  and  $^{13}\text{C}$  chemical shifts, ppm, of various TPT tautomers and derivatives in  $\text{D}_2\text{O}$ , methanol- $d_4$  and  $\text{DMSO}-d_6$  solutions

	TPT $\times$ HCl <sup>a</sup> Lactone $\text{D}_2\text{O}$ , pH 6	TPT $\times$ HCl <sup>b</sup> Carboxylate $\text{D}_2\text{O}$ , pH 10	TPT <sup>c</sup> Free base	TPT <sup>d</sup> Ether 23- $\text{CH}_2\text{OCH}_3$	TPT <sup>e</sup> Lactone $\text{DMSO}-d_6$	TPT <sup>e</sup> Carboxylate $\text{DMSO}-d_6$	TPT <sup>f</sup> Alcohol $\text{DMSO}-d_6$
2-C	150.8	148.5	148.9	147.3	150.2	149.6	149.5
3-C	147.9	146.9	148.0	148.4	146.1	146.6	146.4
5- $\text{CH}_2$	5.20; 53.4	5.04; 53.4	5.25; 51.2	5.23; 51.3	5.28, 50.6	5.26, 50.7	5.25; 50.8
6-C	133.0	n.o.	n.o.	n.o.	131.2	130.3	130.1
7-CH	8.65; 128.5	8.25; 126.0	8.61; 126.4	8.52; 127.0	8.91, 126.8	8.75, 127.7	8.75; 127.9
8-C	131.5	132.4	130.6	132.3	n.o.	129.5	129.6
9-C	110.8	109.9	113.3	115.8	109.1	109.4	119.6
10-C	160.5	169.4	162.4	165.1	n.o.	n.o.	154.2
11-CH	7.47; 125.4	7.25; 131.1	7.36; 126.4	7.36; 128.9	7.64, 122.5	7.49, 123.0	7.48; 123.2
12-CH	7.94; 134.6	7.85; 133.3	7.95; 131.0	7.87; 130.8	8.19, 133.5	7.97, 130.5	7.96; 130.6
13-C	145.3	143.7	144.6	143.9	144.0	144.2	144.1
14-CH	7.37; 101.2	7.50; 103.5	7.60; 98.7	7.59; 98.3	7.29, 96.6	7.25, 96.2	7.25; 96.5
15-C	153.4	159.7	153.0	153.0	150.7	n.o.	150.6
16-C	120.9	129.0	119.2	118.5	119.2	119.0	118.6
16a-C(O)	n.o.	165.2	159.5	159.5	157.5	n.o.	157.3
17- $\text{CH}_2$	5.37, 5.50; 68.4	4.84; 58.7	5.37, 5.57; 66.7	5.37, 5.57; 66.7	5.29, 5.42; 65.6	5.40, n.o.	5.39; 65.7
18- $\text{CH}_2$	1.96, 33.5	2.20, 2.38; 34.2	1.96; 32.6	1.96; 32.6	1.86; 30.7	1.38, 26.3	1.84; 30.7
19- $\text{CH}_3$	0.96; 9.6	1.07; 10.2	1.01; 8.15	1.01; 8.15	0.87, 8.2	0.82, n.o.	0.86; 8.3
C-20	76.2	82.2	74.3	74.3	73.0	n.o.	72.9
21-C(O)	177.4	181.1	175.1	175.1	173.1	n.o.	173.0
22- $\text{CH}_3(\text{N})$	2.91; 45.1	2.85; 44.5	2.49; 44.5	–	2.84, 43.0	n.o.	–
23- $\text{CH}_2$	4.68; n.o.	4.51; 56.7	4.19; 56.7	4.98; 66.3	4.72, 51.0	4.95, 53.9	4.94; 54.2
Other	–	–	–	$\text{OCH}_3$ 3.44; 57.8	–	–	–

<sup>a</sup>  $\text{D}_2\text{O}$  solution pH = 6.<sup>b</sup>  $\text{D}_2\text{O}$  solution pH = 10.<sup>c</sup> Obtained from TPT  $\times$  HCl, see Experimental section, in  $\text{DMSO}-d_6$  solution.<sup>d</sup> Product of the reaction on gel using ethyl acetate:  $\text{CH}_3\text{OH}$  eluent,  $\text{CD}_3\text{OD}$  solvent.<sup>e</sup>  $\text{DMSO}-d_6$ .<sup>f</sup> Product of quaternization reaction, see Scheme 4,  $\text{DMSO}-d_6$ .

$4.4 \times 10^{-3}$  mmol) was dissolved in  $\text{H}_2\text{O}$  (0.5 ml) and pH was set to 7 using  $\text{NaHCO}_3$  aqueous solution. Free TPT was extracted with  $\text{CH}_2\text{Cl}_2$  and dried under vacuum.

## Reaction procedures

### General procedure of TPT reaction on silica gel

TPT hydrochloride (2 mg,  $4.4 \times 10^{-3}$  mmol) was dissolved in  $\text{CH}_3\text{OH}$  (1 ml), applied to a PLC glass plate (silica gel, 2 mm) and dipped into a mixture of  $\text{CH}_3\text{OH}$  and  $\text{CH}_3\text{CO}_2\text{Et}$  (1 : 9, v/v). Two fractions were collected and eluted from gel with  $\text{CH}_3\text{OH}$ . Fraction with  $R_f = 0.7$  was recognized as impurities while the one with  $R_f = 0.1$  as a methyl ether, 23- $\text{CH}_2\text{OCH}_3$ ,  $\text{C}_{22}\text{H}_{21}\text{N}_2\text{O}_6$ .

**$^1\text{H NMR}$**  ( $\text{CD}_3\text{OD}$ ):  $\delta = 1.01$  (t, 3H,  $J = 7$  Hz), 1.96 (q, 2H,  $J = 7$  Hz), 3.44 (s, 3H), 4.98 (s, 2H), 5.22 (residual signal because of deuteration), 5.37 (d, 1H,  $J = 16$  Hz), 5.55 (d, 1H,  $J = 16$  Hz), 7.36 (d, 1H,  $J = 9$  Hz), 7.59 (s, 1H), 7.87 (d, 1H,  $J = 9$  Hz), 8.54 (s, 1H).

**HR-MS** (ESI): Calculated for  $\text{C}_{22}\text{H}_{20}\text{N}_2\text{O}_6$ ,  $[\text{M} - \text{H}]^+$  407.1237, found: 407.1231.

### Reaction in methanol

TPT hydrochloride (0.5 mg,  $1.1 \times 10^{-3}$  mmol) was dissolved in  $\text{CD}_3\text{OD}$  (0.7 ml) and incubated at  $4^\circ\text{C}$  for 10 days. Product of this reaction was identified as an ether  $\text{C}_{22}\text{H}_{18}\text{D}_3\text{N}_2\text{O}_6$ .

**$^1\text{H NMR}$**  ( $\text{CD}_3\text{OD}$ ), just after dissolving:  $\delta = 1.01$  (t, 3H,  $J = 7$  Hz), 1.96 (q, 2H,  $J = 7$  Hz), 2.90 (s, 6H), 4.74 (s, 2H), 5.35 (bs, 2H), 5.38 (d, 1H,  $J = 16$  Hz), 5.59 (d, 1H,  $J = 16$  Hz), 7.57 (d, 1H,  $J = 9$  Hz), 7.64 (s, 1H), 8.21 (d, 1H,  $J = 9$  Hz), 8.81 (s, 1H).

**$^1\text{H NMR}$**  ( $\text{CD}_3\text{OD}$ ) after 10 days:  $\delta = 1.01$  (t, 3H,  $J = 7$  Hz), 1.96 (q, 2H,  $J = 7$  Hz), 2.68 (s, 6H =  $(\text{CH}_3)_2\text{N} \times \text{HCl}$ ), 5.00 (s, 2H), 5.31 (bs, 0.5 H, partly deuterated), 5.38 (d, 1H,  $J = 16$  Hz), 5.58 (d, 1H,  $J = 16$  Hz), 7.47 (d, 1H,  $J = 9$  Hz), 7.63 (s, 1H), 8.03 (d, 1H,  $J = 9$  Hz), 8.74 (s, 1H).

The aromatic part of the spectrum differs from that obtained after the reaction of TPT on silica, most probably due to the deuteration of a methyl group and/or due to the differences in pH and concentration of the sample.

**HR-MS** (ESI): Calculated for  $\text{C}_{22}\text{H}_{19}\text{D}_3\text{N}_2\text{O}_6$ ,  $[\text{M} + \text{H}]^+$  412.1582, found: 412.1664.

### General procedures for alkylation of TPT

#### $\text{CF}_3\text{SO}_3\text{CH}_3$ (methyl trifluoromethanesulfonate)

Methyl trifluoromethanesulfonate (0.1 ml, 0.9 mmol) was dissolved in  $\text{CH}_2\text{Cl}_2$  (3 ml) and then small amount of  $\text{K}_2\text{CO}_3$  was added. The mixture was stirred for 30 min to neutralize possible formation of trifluoromethanesulfonic acid ( $\text{CF}_3\text{SO}_3\text{H}$ ). The solution was filtered from  $\text{K}_2\text{CO}_3$ , added to dry free TPT (1.8 mg,  $4.4 \times 10^{-3}$  mmol) and stirred for 24 h at room temperature. The mixture was evaporated to dryness under vacuum at room temperature and dissolved



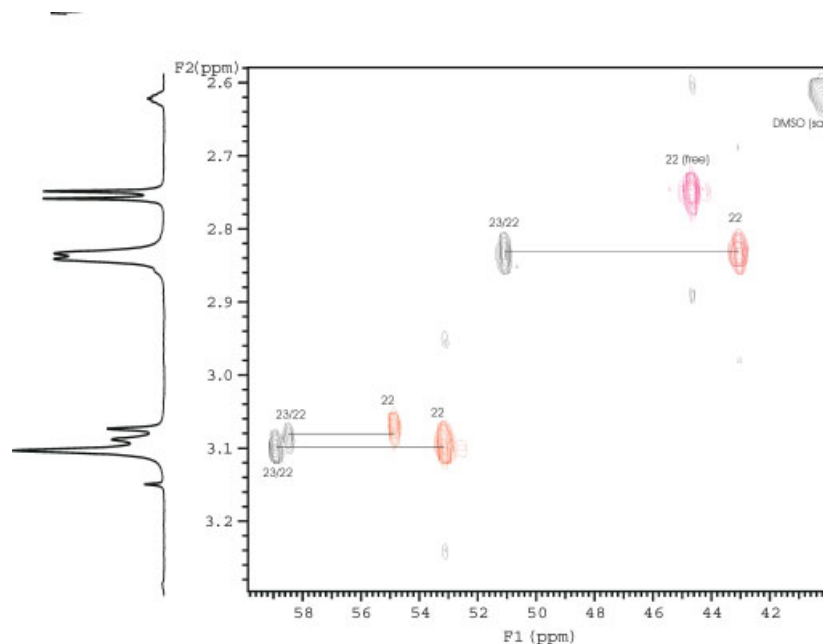


**Figure 4.** The overlay of the aliphatic part of the  $^1\text{H}/^{13}\text{C}$ -HSQCAD-HMBC spectrum (colored/black) of the one of the product mixtures (DMSO- $d_6$  solution) in the quaternization reaction of neutral TPT with  $\text{CF}_3\text{SO}_2\text{OCH}_3$ . The colored HSQCAD signals are linked with the black HMBC peaks evidencing the attachment of respective methyl groups to 23- $\text{CH}_2$  carbon atom. The HSQCAD signal in purple has no correlation and is assigned to a salt.

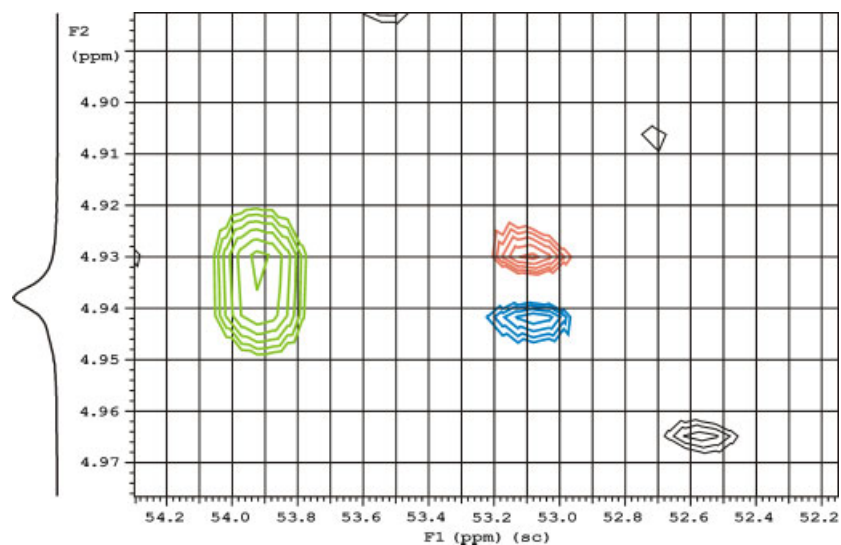


**Figure 5.** Overlay of the 500 MHz phase-sensitive  $^1\text{H}/^{13}\text{C}$ -HMBC trace (blue-red) and absolute value  $^1\text{H}/^{13}\text{C}$ -HSQCAD trace (green) of  $[\text{Me}_3\text{N}^+ \text{CH}_3\text{SO}_3^-]$  salt of TPT in DMSO- $d_6$  solution.  $\text{CH}_3-\text{SO}_2-\text{OCH}_3$  was used for the quaternization reaction.

$^1\text{H}/^{13}\text{C}$ -HSQCAD spectra:<sup>[31]</sup> The echo-antiecho phase-sensitive gradient-selected  $^1\text{H}-^{13}\text{C}$  HSQCAD (heteronuclear single quantum coherence adiabatic version) NMR spectra were obtained with a spectral width of 5000 Hz, 2048 points in the  $^1\text{H}$  dimension and 8000 Hz,  $800 \times 2$  increments in the  $^{13}\text{C}$  dimension; 128 transients per  $t_1$  increment, with a relaxation delay of 1 s and  $^1J(\text{C},\text{H}) = 135$  Hz. The data were linearly predicted to 1600 points and zero filled to 4096 points in  $F_1$  before Fourier transformation.

$^1\text{H}/^{13}\text{C}$ -HMBC: The gradient-selected  $^1\text{H}-^{13}\text{C}$  HMBC spectra were performed with an acquisition time of 0.2 s,  $^1\text{H} - 90^\circ$  pulse width of  $7.8 \mu\text{s}$ ,  $^{13}\text{C} - 90^\circ$  pulse width of  $11.5 \mu\text{s}$ , a spectral width of 5000 Hz, 2048 data points in the  $^1\text{H}$  dimension and 25 000 Hz, 1024 increments in the  $^{13}\text{C}$  dimension, and a relaxation delay of

1.2 s. The data were acquired as absolute value mode, with 64 transients per  $t_1$  increment. The experiment was optimized for  $^nJ(\text{C},\text{H}) = 8$  Hz and low pass filter for  $^1J(\text{C},\text{H}) = 140$  Hz was used. The data were linearly predicted to 2048 points and zero filled to 4096 points in  $F_1$  prior to Fourier transformation.

#### Acknowledgements

The authors acknowledge the financial support during this research from Ministry of Science and Higher Education Grant No. NN204 155736. The authors thank Prof. S. Szymański (Institute of Organic Chemistry, Polish Academy of Sciences) for the detailed spin simulation (Fig. S1). The authors acknowledge the help of Dr K. Zdanowski in preparing the manuscript.

## Supporting information

Supporting information may be found in the online version of this article.

## References

- [1] P. B. Arimondo, G. S. Laco, C. J. Thomas, L. Halby, D. Pez, P. Schmitt, A. Boutorine, T. Garestier, Y. Pommier, S. M. Hecht, J. S. Sun, C. Bailly, *Biochemistry* **2005**, *44*, 4171.
- [2] K. Cheng, N. J. Rahier, B. M. Eisenhauer, R. Gao, S. J. Thomas, S. M. Hecht, *J. Am. Chem. Soc.* **2005**, *127*, 838.
- [3] N. J. Rahier, B. M. Eisenhauer, R. Gao, S. H. Jones, S. M. Hecht, *Org. Lett.* **2004**, *6*, 321.
- [4] A. Cagir, S. H. Jones, R. Gao, B. M. Eisenhauer, S. M. Hecht, *J. Am. Chem. Soc.* **2003**, *125*, 13628.
- [5] P. Pourquier, Y. Pommier, *Adv. Cancer Res.* **2001**, *80*, 189.
- [6] F. Zunino, G. Pratesi, *Expert Opin. Investig. Drugs* **2004**, *13*, 269.
- [7] L. F. Liu, P. Duann, C. T. Lin, P. D'Arpa, J. Wu, *Ann. NY Acad. Sci.* **1996**, *803*, 44.
- [8] C. H. Takimoto, J. Wright, S. G. Arbut, *Biochim. Biophys. Acta* **1998**, *1400*, 107.
- [9] W. J. Slichenmyer, E. K. Rowinsky, R. C. Donehower, S. H. Kaufmann, *J. Natl. Cancer Inst.* **1993**, *85*, 271.
- [10] M. C. Wani, A. W. Nicholas, M. E. Wall, *J. Med. Chem.* **1987**, *30*, 2317.
- [11] C. Jaxel, K. W. Kohn, M. C. Wani, M. E. Wall, Y. Pommier, *Cancer Res.* **1989**, *49*, 1465.
- [12] R. P. Hertzberg, M. J. Caranfa, S. M. Hecht, *Biochemistry* **1989**, *28*, 4629.
- [13] R. P. Hertzberg, M. J. Caranfa, K. G. Holden, D. R. Jakas, G. Gallagher, M. R. Mattern, S. M. Mong, J. O. Bartus, R. K. Johnson, W. D. Kingsbury, *J. Med. Chem.* **1989**, *32*, 715.
- [14] Y. Pommier, G. Kohlhagen, K. W. Kohn, F. Leteurtre, M. C. Wani, M. E. Wall, *Proc. Natl. Acad. Sci. U.S.A.* **1995**, *92*, 8861.
- [15] L. P. Rivory, J. Robert, *Bull. Cancer* **1995**, *82*, 265.
- [16] M. R. Redinbo, L. Stewart, P. Kuhn, J. J. Champoux, W. G. Hol, *Science* **1998**, *279*, 1504.
- [17] W. Bocian, R. Kawęcki, E. Bednarek, J. Sitkowski, A. Pietrzyk, M. P. Williamson, P. E. Hansen, L. Kozerski, *Chem. Eur. J.* **2004**, *10*, 5776.
- [18] W. Bocian, R. Kawęcki, E. Bednarek, J. Sitkowski, M. P. Williamson, P. E. Hansen, L. Kozerski, *Chem. Eur. J.* **2008**, *14*, 2788.
- [19] S. Streltsov, V. Oleinikov, M. Ermishov, K. Mochalov, A. Sukhanova, Y. Nechipurenko, S. Grokhovsky, A. Zhuze, M. Pluot, I. Nabiev, *Biopolymers* **2003**, *72*, 442.
- [20] N. A. de Vries, M. Ouwehand, T. Buckle, J. H. Beijnen, O. van Tellingen, *Biomed. Chromatogr.* **2007**, *21*, 1191.
- [21] N. R. Srinivas, *Biomed. Chromatogr.* **2009**, *23*, 447.
- [22] K. Stott, J. Stonehouse, J. Keeler, T.-L. Hwang, A. J. Shaka, *J. Am. Chem. Soc.* **1995**, *117*, 4199.
- [23] T. Thanh Danh, W. Bocian, L. Kozerski, P. Szczukiewicz, J. Frelek, M. Chmielewski, *Eur. J. Org. Chem.* **2005**, 429.
- [24] M. P. Williamson, *Mag. Reson. Chem.* **1987**, *25*, 356.
- [25] R. Aiyama, H. Nagai, S. Sawada, T. Yokokura, H. Itokawa, M. Nakanishi, *Chem. Pharm. Bull.* **1992**, *40*, 2810.
- [26] N. Sanna, G. Chillemi, A. Grandi, S. Castelli, A. Desideri, V. Barone, *J. Am. Chem. Soc.* **2005**, *127*, 15429.
- [27] N. Sanna, G. Chillemi, L. Gontrani, A. Grandi, G. Mancini, S. Castelli, G. Zagotto, C. Zazza, V. Barone, A. Desideri, *J. Phys. Chem. B* **2009**, *113*, 5369.
- [28] S. Sawada, S. Okajima, R. Aiyama, K. Nokata, T. Furuta, T. Yokokura, E. Sugino, K. Yamaguchi, T. Miyasaka, *Chem. Pharm. Bull.* **1991**, *39*, 1446.
- [29] S. Dallavalle, T. Delsoldato, A. Ferrari, L. Merlini, S. Penco, N. Carenini, P. Perego, M. De Cesare, G. Pratesi, F. Zunino, *J. Med. Chem.* **2000**, *43*, 3963.
- [30] W. D. Kingsbury, J. C. Boehm, D. R. Jakas, K. G. Holden, S. M. Hecht, G. Gallagher, M. J. Caranfa, F. L. McCabe, L. F. Faucette, R. K. Johnson, R. P. Hertzberg, *J. Med. Chem.* **1991**, *34*, 98.
- [31] M. F. Summers, L. G. Marzilli, A. Bax, *J. Am. Chem. Soc.* **1986**, *108*, 4285.